Hydrodynamics of prey capture in sharks: effects of substrate

Sandra Nauwelaerts, Cheryl Wilga, Christopher Sanford and George Lauder

References	**This article cites 12 articles, 3 of which can be accessed free** http://rsif.royalsocietypublishing.org/content/4/13/341.full.html#ref-list-1 Article cited in: **http://rsif.royalsocietypublishing.org/content/4/13/341.full.html#related-urls**
Email alerting service	Receive free email alerts when new articles cite this article - sign up in the box at the top right-hand corner of the article or click **here**

To subscribe to *J. R. Soc. Interface* go to: **http://rsif.royalsocietypublishing.org/subscriptions**

REPORT

Hydrodynamics of prey capture in sharks: effects of substrate

**Sandra Nauwelaerts[1,*], Cheryl Wilga[1],
Christopher Sanford[2] and George Lauder[3]**

[1]*Department of Biological Sciences, University of
Rhode Island, Kingston, RI 02881, USA*
[2]*Department of Biology, 114 Hofstra University,
Hempstead, NY 11549, USA*
[3]*Department of Organismic and Evolutionary Biology,
Harvard University, Cambridge, MA 02138, USA*

In suction feeding, a volume of water is drawn into the
mouth of a predator. Previous studies of suction
feeding in fishes have shown that significant fluid
velocities are confined to a region within one mouth
width from the mouth. Therefore, the predator must
be relatively close to the prey to ensure capture
success. Here, theoretical modelling is combined with
empirical data to unravel the mechanism behind
feeding on a substrate. First, we approached the
problem theoretically by combining the stream func-
tions of two sinks. Computational fluid dynamics
modelling is then applied to make quantitative
predictions regarding the effects of substrate proximity
on the feeding hydrodynamics of a benthic shark. An
oblique circular cylinder and a shark head model were
used. To test the models, we used digital particle
image velocimetry to record fluid flow around the
mouth of white-spotted bamboo sharks, *Chiloscyllium
plagiosum*, during suction feeding on the substrate and
in the water column. Empirical results confirmed the
modelling predictions: the length of the flow field can
be doubled due to passive substrate effects during prey
capture. Feeding near a substrate extends the distance
over which suction is effective and a predator strike
can be effective further from the prey.

**Keywords: hydrodynamics; feeding; shark;
digital particle velocimetry; modelling**

1. INTRODUCTION

Suction feeding is a foraging strategy employed by the
majority of aquatic vertebrates (Lauder & Shaffer

*Author and address for correspondence: Ocean Ecosystems,
University of Groningen, 9750 AA Haren, The Netherlands
(s.nauwelaerts@rug.nl).

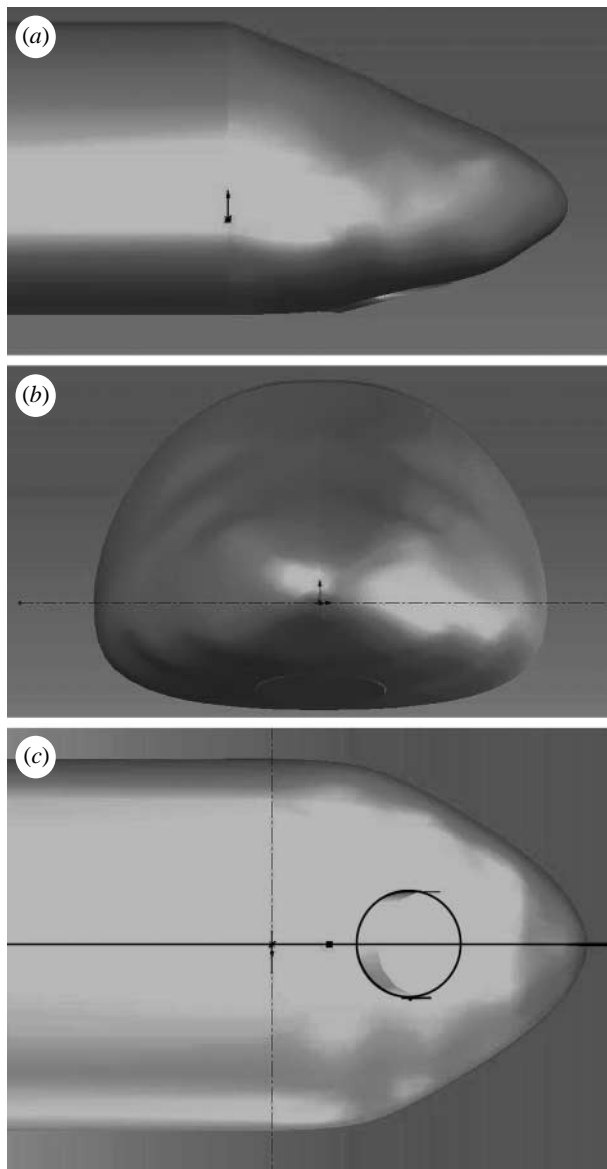1993). It involves rapidly expanding the oral cavity to
direct a flow of water containing prey into the mouth
(Muller *et al.* 1982; Muller & Osse 1984; Lauder &
Shaffer 1993; Aerts *et al.* 2001). Flow velocity is key to
foraging success because increasing velocity produces a
concomitant increase in the distance over which prey
are captured (Muller *et al.* 1982; Day *et al.* 2005; Van
Wassenbergh *et al.* 2006). Previous models (Muller
et al. 1982; Van Leeuwen & Muller 1984) and
experiments of suction feeding in fish (Ferry-Graham
et al. 2003; Day *et al.* 2005) have demonstrated that
significant flow velocities are confined to a region within
one mouth diameter of the oral cavity. Therefore, the
predator must be relatively close to the prey to ensure
capture success (Muller *et al.* 1982). While fish appear
to be somewhat constrained by the hydrodynamics of
suction feeding, there is potential to improve foraging
effectiveness through external means, for example by
using the substrate to concentrate flow in a relatively
two-dimensional, rather than three-dimensional space
(Alexander 1967). Other organisms are known to use
substrate-mediated fluid dynamics to improve loco-
motor performance (e.g. ground effect in birds; Rayner
1991). In contrast to the thoroughly studied field of
suction feeding in bony fishes in the water column, the
ability of organisms to use substrates to enhance
feeding performance has not been investigated.

An excellent model species to study the effects of the
substrate on the hydrodynamics of suction feeding are
white-spotted bamboo sharks, *Chiloscyllium plagiosum*
(Bennett 1830). This common, but little-studied,
inshore shark inhabits benthic environments around
coral reefs (Michael 2003) and is a strong suction feeder
(Wilga & Sanford 2003). It usually feeds on bottom
dwelling marine invertebrates (Compagno, 1984).

In this paper, theoretical modelling is combined with
empirical data to unravel the mechanism behind
feeding on the substrate. First, we approached the
problem theoretically by combining the stream func-
tions of two sinks. This way, we are able to provide an
analytical explanation on the nature of the substrate
effect. However, due to the assumptions of such a
theoretical model, this cannot be used as an absolute
predictive model. Therefore, computational fluid
dynamics (CFD) modelling is applied in order to
make quantitative predictions regarding the effects of
substrate proximity on the feeding hydrodynamics of a
benthic shark. We constructed two three-dimensional
CFD models: (i) a simplified oblique circular cylinder to
determine the effect of the substrate, and (ii) a realistic
shark head to determine the additional effect of the
head morphology. To test these models, we used digital
particle velocimetry (DPIV) to record fluid flow around
the mouth of bamboo sharks during suction feeding on
the substrate and in the water column.

2. MATERIAL AND METHODS

2.1. Theoretical fluid mechanics

For an incompressible, inviscid flow, stream functions
have been proven useful. To predict the effect of a wall
on flow velocities, we superposed the elementary flows
of two sinks placed at a distance $2a$ from each with the

Figure 1. Shark head model in three views: (*a*) a lateral, (*b*) a frontal and (*c*) a ventral view.
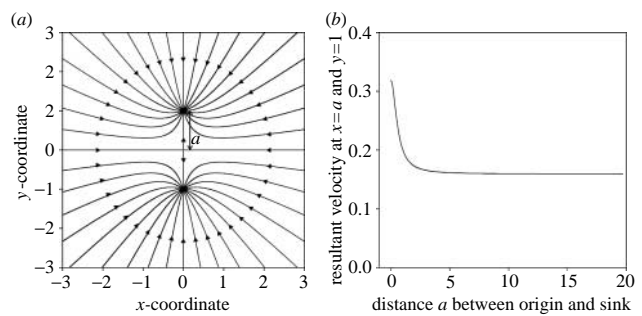

Figure 2. (*a*) Streamline pattern for two sinks at a distance 2*a*. (*b*) A plot of v_R for a chosen position from sink 1 against distance *a*. The smaller *a*, and the closer together the two sinks, the higher v_R up to a doubling of the asymptotic v_R.
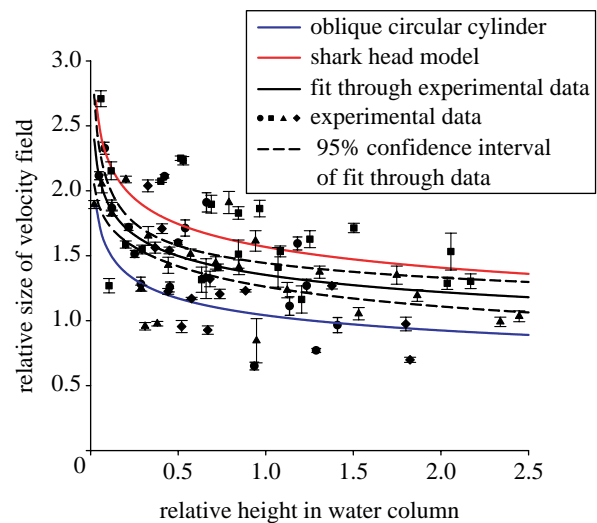

Figure 3. Effect of the substrate proximity (expressed in relative height from the substrate) on the size of the velocity field (expressed as the relative distance from the mouth to the boundary of the fluid velocity region). Units are in mouth widths. Black symbols represent 78 data points from four individuals (individual 1, $N=17$, circles; individual 2, $N=22$, squares; individual 3, $N=4$, triangles; individual 4, $N=15$, diamond). A power function was fitted through the data points (black line), and through the predictions of the oblique circular cylinder model (blue line) and the shark head model (red line).

origin of the coordinate system in the middle of the two sinks. We plotted the velocity change with increasing *a* for a position at a fixed distance from one of the sinks to assess the effect of *a* on the velocity profile.

2.2. Computational fluid dynamics models

Two models were built-in SolidWorks 2006: one simple oblique circular cylinder of 20 mm diameter; and one model shaped after bamboo shark head dimensions (figure 1). In both cases, a horizontal substrate was added to the assembly. The inflow velocity was chosen based on preliminary DPIV data (see below) and was set at $0.5\,\mathrm{m\,s^{-1}}$. Using FloWorks 2006, the three-dimensional flow velocity distribution around the 'mouths' of the two models was calculated for the first 0.10 s of flow generation. After this time period, the distance from the mouth to the iso-velocity line of $0.05\,\mathrm{m\,s^{-1}}$ in front of the mouth was measured as a metric for the size of the fluid velocity field.

These simulations were performed with the substrate placed at different heights from the mouth (0–50 in 1 mm intervals) for both models. Both the height and the fluid velocity field size were normalized to mouth diameter (20 mm). A power plot was fitted through the predictions of both models.

2.3. Animals

Four white-spotted bamboo sharks, *C. plagiosum* (68–72 cm TL), were obtained from SeaWorld of San Diego. The animals were housed in 3028 l aquaria at 24.4°C and maintained on a diet of squid and silverside fish. The animals were trained to eat squid from a wooden skewer held horizontally at different heights in the water column.
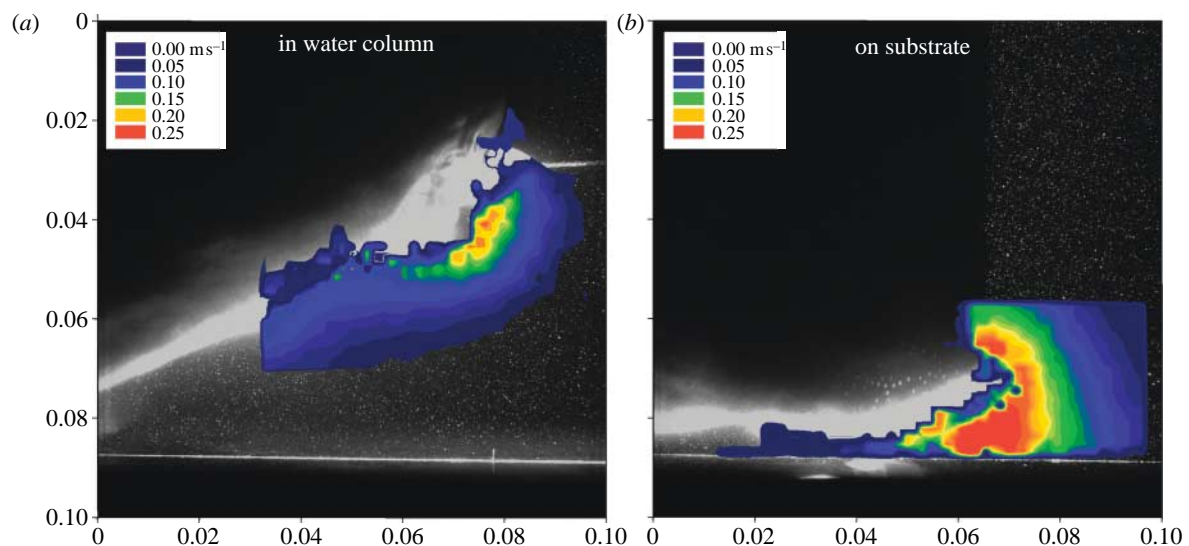
Figure 4. A representative DPIV vector magnitude plot of a suction feeding shark (*a*) in the water column and (*b*) on the substrate.

2.4. Digital particle velocimetry

The animals were transferred from the housing tank to a 151 l glass tank. The sharks lay on the substrate while 1 cm^2 square pieces of squid were offered at various heights from the substrate.

To visualize the flow generated by the suction feeding shark, the salt water of the experimental tank was seeded at a density of 6.6 mg l^{-1} with silver coated, near neutrally buoyant reflective particles (Potter Ind., 12 µm diameter). A light beam from a continuous 5W argon-ion laser was focused into a vertical sheet of 2 mm thick and 10 cm wide and illuminated a section around the shark head. A high speed, high resolution (1024 × 1024 pixels) Photron APX camera was placed perpendicular to the laser sheet and recorded movements of the particles at 500 frames per second.

2.5. Digital particle velocimetry analysis

After DPIV data acquisition, the images were processed using DaVis v. 6.2.4 software using a sequential cross-correlation without pre-processing. An initial correlation window of 64 × 64 pixels was selected with multi-pass with decreasing smaller size to a final interrogation window of 32 × 32 pixels with 50% overlap. Vector validation was performed, rejecting any vectors whose magnitude fell further than two standard deviations from the mean. Rejected vectors were replaced by those interpolated from surrounding vectors. The resulting vector magnitude plot was displayed over the original recordings and colour coded such that significant vectors were red, vectors at the threshold of 5 cm s^{-1} were white and vectors under this threshold were blue and considered insignificant to the flow.

For each sequence, four magnitude plots at the moment of highest flow velocities were exported as bitmaps and digitized in SigmaScan Pro v. 4.01. The distances from the mouth (more specifically, from the middle of the narrowed section of flow going into the mouth—the middle of the 'stalk' of the mushroom shaped velocity field) to the iso-velocity region at 5 cm s^{-1} and the height of the mouth from the substrate were measured. The height and the fluid velocity field size were normalized to the mouth diameter of each individual.

2.6. TTP and angle mouth aperture

Time to peak gape (TTP) was measured on the DPIV video files and used as a measure for effort. The shorter the time it takes for the mouth cavity to get fully expanded, the greater the effort (assuming the mouth kinematics are similar; Sanford & Wainwright 2002). In addition, at the moment of largest fluid velocity region, the angle of the mouth aperture to the substrate was measured.

2.7. Statistics

After log transformation of the experimental data, a repeated measures ANCOVA with individual as random factor and height as a covariable was performed. The 95% confidence interval of the regression line of size of the fluid velocity region against height was calculated and plotted with the theoretical predictions of the CFD models. To test the validity of the CFD models, a χ^2-test in Statistica v. 6.1 was performed using the predictive function of the model as predicted values and the experimental data as observed. Also the slopes and intercepts of the models were compared with the experimental data on log-transformed data in a linear regression model in GraphPad Prism 4.

The log transformed mouth aperture angles were regressed against height in the water column, again while accounting for individual effects in Statistica v. 6.1. Similarly, the size of the fluid velocity region was regressed against TTP.

3. RESULTS

3.1. Theoretical fluid mechanics

The stream function after superposition of two sinks placed at $(0, a)$ and $(0, -a)$ is:

$$\psi = \frac{-m}{2\pi}\tan^{-1}\left(\frac{x}{y-a}\right) + \frac{-m}{2\pi}\tan^{-1}\left(\frac{x}{y+a}\right), \quad (3.1)$$

where m is the strength of the sink, a is the distance from the sink to the origin of the coordinate system and x and y are the x- and y-coordinates, respectively.

The streamline pattern for a sink–sink pair is shown in figure 2*a*.

The velocity components u (in x-direction) and v (in y-direction) are therefore,

$$u = \frac{-m}{2\pi}\left[\left(\frac{y-a}{(y-a)^2 + x^2}\right) + \left(\frac{y+a}{(y+a)^2 + x^2}\right)\right], \quad (3.2)$$

and

$$v = \frac{-m}{2\pi}\left[\left(\frac{x}{(y-a)^2 + x^2}\right) + \left(\frac{x}{(y+a)^2 + x^2}\right)\right], \quad (3.3)$$

and the resultant velocity v_R becomes

$$v_R = \sqrt{u^2 + v^2}. \quad (3.4)$$

Using these equations, v_R at a fixed distance from one of the sinks could be calculated in function of a (figure 2*b*).

3.2. Computational fluid dynamics models

The first model consisted of a circular cylinder placed obliquely in respect to the horizontal surface to mimic the angle of the mouth opening. Adding a substrate, a purely passive effect, caused a doubling of the distance from the mouth to the threshold velocity (figure 3). The effect of the substrate using the shark head model was similar, except the intercept of the distance versus height line is higher. Thus, the shark head morphology increases the distance between the mouth and the threshold velocity by an additional 50% (figure 3).

3.3. Experimental digital particle velocimetry data

The experimental data confirm the modelling predictions (figure 3). The power fit through the experimental data with its 95% confidence interval falls in between the plotted predictive equations of the two models (figure 3). A repeated measures ANCOVA shows a significant effect of height in the water column on the size of the fluid velocity region, expressed as a distance ($p = 0.01$). The effect of the substrate is also a doubling of the distance in the experimental data (figure 4). A significant individual effect on distance was found, which suggests that individuals differ in the strength of their suction flow. However, the statistical interaction effect of individual and height was not significant, this means that the influence of the substrate was similar for all individuals. Both CFD models were accurate in their prediction of the effect of the substrate on the size of the fluid velocity region: the slopes did not differ significantly from each other or from the experimental data. The intercepts, however, did differ significantly: the cylinder showed an underestimation of the distance; the shark head model overestimated the distance.

3.4. TTP and mouth aperture

TTP was not significantly correlated to fluid velocity region size ($p = 0.61$). Mouth aperture angle did significantly change with height in the water column for three out of four animals. The difference amounted to 20° (approx. 20–40° with the substrate).

4. DISCUSSION

Simple two-dimensional fluid mechanics predict that velocity at a fixed distance from a sink will increase when a second sink is moved closer, which indicates that a substrate close to a suction feeding animal may be beneficial. Indeed, an increase in velocity at a given position means an increase in the affected distance in the direction between source and the chosen position. The larger this distance, the further away the predator can be from the prey and the better the chances are that a predator can overcome drag on the prey and generate enough suction to draw the prey into the mouth. However, a sink is a flow pattern in the xy-plane to which flow is radially inward and the origin of a sink is a singular point. Thus, while an actual flow may resemble a sink for some values, it has no exact physical counterpart (Fox & McDonald 1985). Therefore, the next step to more realistic predictions was to undertake CFD modelling. The cylinder predicted the effect of the substrate on the hydrodynamics, while the shark head model added the effect of the head morphology. For the cylinder model, the proximity of a substrate causes up to a doubling of the distance between the mouth and the chosen threshold velocity. The shape of the shark head adds an additional 50% to the increase of this distance. DPIV results revealed that sharks feeding in the water column generated significant flow velocities over a relatively small distance—within one mouth diameter—in accordance with previous studies (Muller *et al.* 1982; Van Leeuwen & Muller 1984; Ferry-Graham *et al.* 2003; Day *et al.* 2005). In contrast, sharks foraging in close proximity to the substrate, amplified the distance over which suction occurred by up to 2.5 times due to passive hydrodynamic effects, as predicted by the theoretical calculations and the CFD models. This effect is magnified by the active change in mouth aperture angle by the shark (smaller angle at the substrate). The increase in suction distance is not due to an increase in effort by the shark, as shown by the lack of correlation between effort and distance, but is instead clearly correlated to the height in the water column.

The model of the shark head overestimates the size of the affected volume somewhat. This is probably due to an overestimation of the water velocity entering the mouth. The velocity of $0.5\ \mathrm{m\ s^{-1}}$ was chosen based on preliminary average DPIV data. The vectors calculated close to the animal, however, are usually more prone to body effects than the velocities calculated further from

the body. Ideally, a DPIV image consists of a black image homogeneously filled with white dots. Objects, such as a shark head, tend to reflect glare from the laser, causing the background of the image to become less dark. In addition, although the shark propped the body off the substrate with the pectoral fins, the head sometimes moved slightly forward due to the incoming water momentum. This creates additional uncertainties on the measured water velocities right in front of the mouth of the shark. Also, the inlet velocity was kept constant in the model. In reality, the velocity is zero when the shark starts opening the mouth and increases exponentially to a maximal velocity. In spite of these simplifications in the models, the predictive power of the models is convincing.

In conclusion, feeding near a substrate, particularly when combined with a long pre-oral snout, extends the distance over which suction is effective. This feeding strategy appears to benefit benthic animals by increasing the strike radius and by reducing the degree of accuracy necessary to capture prey successfully. Future research will focus on how animals optimize this strategy by looking at the hydrodynamics of suction feeders in a wide range of ecological niches.

REFERENCES

Aerts, P., Van Damme, J. & Herrel, A. 2001 Intrinsic mechanics and control of fast cranio-cervical movements in aquatic feeding turtles. *Am. Zool.* **41**, 1299–1310. (doi:10.1668/0003-1569(2001)041[1299:IMACOF]2.0.CO;2)

Alexander, R. McN. 1967 Functions and mechanisms of protrusible upper jaws of some acanthopterygian fish. *J. Zool.* **151**, 43–57.

Compagno, L. J. V. 1984 FAO species catalog. Sharks of the world. An annotated and illustrated catalogue of sharks species known to date. Part 1. Hexanchiformes to Lamniformes. FAO Fish Synop. 125 vol. 4.

Day, S. W., Higham, T. E., Cheer, A. Y. & Wainwright, P. C. 2005 Spatial and temporal patterns of water flow generated by suction-feeding bluegill sunfish *Lepomis macrochirus* resolved by particle image velocimetry. *J. Exp. Biol.* **208**, 2661–2671. (doi:10.1242/jeb.01708)

Ferry-Graham, L. A., Wainwright, P. C. & Lauder, G. V. 2003 Quantification of flow during suction feeding in bluegill sunfish. *Zoology* **106**, 159–168. (doi:10.1078/0944-2006-00110)

Fox, R. W. & McDonald, A. T. 1985 *Introduction to fluid mechanics.* New York, NY: Wiley.

Lauder, G. V. & Shaffer, H. B. 1993 Design of feeding systems in aquatic vertebrates: major patterns and their evolutionary interpretations. In *The skull*, vol. 3 (eds J. Hanken & B. K. Hall), pp. 113–149. Chicago, IL: University of Chicago Press.

Michael, S. W. 2003 *Reef sharks & rays of the world.* Monterey, CA: Sea Challengers.

Muller, M. & Osse, J. W. M. 1984 Hydrodynamics of suction feeding in fish. *Trans. Zool. Soc.* **37**, 51–135.

Muller, M., Osse, J. W. M. & Verhagen, J. H. G. 1982 A quantitative hydrodynamical model of suction feeding in fish. *J. Theor. Biol.* **95**, 49–79. (doi:10.1016/0022-5193(82)90287-9)

Rayner, J. M. 1991 On the aerodynamics of animal flight in ground effect. *Phil. Trans.: Biol. Sci.* **334**, 119–128.

Sanford, C. P. J. & Wainwright, P. C. 2002 Use of sonomicrometry demonstrates the link between prey capture kinematics and suction pressure in largemouth bass. *J. Exp. Biol.* **205**, 3445–3457.

Van Leeuwen, J. L. & Muller, M. 1984 Optimum sucking techniques for predatory fish. *Trans. Zool. Soc.* **37**, 137–169.

Van Wassenbergh, S., Aerts, P. & Herrel, A. 2006 Hydrodynamic modelling of aquatic suction performance and intra-oral pressures: limitations for comparative studies. *J. R. Soc. Interface* **3**, 507–514. (doi:10.1098/rsif.2005.0110)

Wilga, C. D. & Sanford, C. P. 2003 Suction generation in bamboo sharks. *Integr. Comp. Biol.* **43**, 979.